Available online at www.sciencedirect.com
SCIENCE DIRECT®
Journal of Nuclear Materials 336 (2005) 47–53
journal of nuclear materials
www.elsevier.com/locate/jnucmat

Corrosion behavior of Inconel 690 and 693 in an iron phosphate melt

Dongmei Zhu [a], Cheol-Woon Kim [b,*], Delbert E. Day [b]

[a] State Key Laboratory of Solidification Processing, Northwestern Polytechnical University, Xi'an, Shaanxi 710072, PR China
[b] Graduate Center for Materials Research, University of Missouri-Rolla, 101 Straumanis Hall, Rolla, MO 65409-1170, USA

Received 12 May 2004; accepted 17 August 2004

Abstract

The corrosion resistance of Inconel 690 and 693 coupons submerged in an iron phosphate melt has been investigated. After 155 days in an iron phosphate melt at 1050 °C, which contained 30 wt% of a simulated low activity waste (LAW at Hanford), the weight loss of Inconel 690 and 693 was 14% and 8%, respectively. The overall corrosion rate, calculated from the initial and final dimensions of each coupon, was 1.3 and 0.7 μm/day for the Inconel 690 and 693, respectively. Scanning electron microscopy and X-ray diffraction of the submerged Inconel coupons after 155 days in the iron phosphate melt showed that an altered surface layer had formed which was depleted in nickel and consisted of a $(Fe, Cr)_2O_3$ solid solution. This altered layer appears to be chemically protective as indicated by the gradual reduction in weight loss which occurred with time in the iron phosphate melt. Inconel 693 appears to be a better candidate to use as an electrode in iron phosphate melts since its corrosion rate and weight loss was only about one half that of Inconel 690.

PACS: 28.41.Kw; 60.80

1. Introduction

The US Department of Energy (DOE) Hanford Site in Washington State has more than 55 million gallons of radioactive waste stored in 177 underground storage tanks [1]. It is planned to retrieve this waste from the tanks and separate it into a low activity waste (LAW) and a high level waste (HLW) which will be separately vitrified in the Hanford Tank Waste Treatment Plant. Noteworthy compositional features of the Hanford LAW is that it contains significant amounts of sodium, sulfate, and phosphate [2–4], all of which can limit the maximum waste loading in a borosilicate glass, the only glass currently approved by DOE, to below 10 wt% [5]. The maximum LAW loading in a borosilicate glass is largely determined by the amount of sulfate in the waste [2,6–8]. If the LAW waste loading was not limited by the amount of sulfate which a borosilicate glass can contain, then the waste loading could be increased up to 35 wt% and the amount of glass produced at Hanford could be reduced by as much as 43% [3].

Previous work [3,4,9] has suggested several advantages for vitrifying the Hanford LAW in an iron phosphate glass. The most important is the higher waste loading (up to 35 wt%) of the simulated LAW with no

* Corresponding author. Tel.: + 1 573 341 4359; fax: + 1 573 341 2071.
E-mail address: cheol@umr.edu (C.-W. Kim).

0022-3115/$ - see front matter © 2004 Elsevier B.V. All rights reserved.
doi:10.1016/j.jnucmat.2004.08.010

indication of sulfate salt segregation, as seen in most borosilicate glasses. It is unlikely that the LAW waste loading in iron phosphate glasses will be limited by the SO_3 content of the LAW. Another advantage is that iron phosphate glasses containing LAW simulant can be melted at temperatures as low as 1000–1050 °C. Iron phosphate melts also have a high fluidity (200–900 centipoise) at their melting temperature so they rapidly become homogeneous, which reduces their melting times to as short as a few hours (<4 h) compared to the >48 h residence time for the borosilicate melts in the Joule Heated Melter (JHM) at the Defense Waste Processing Facility (DWPF), Westinghouse Savannah River Co.

Experience in melting iron phosphate glasses in the US is limited. Several hundred iron phosphate compositions have been melted without problems in ordinary refractories, but the largest melts were less than 50 kg. No attempts have been made to melt iron phosphate glasses on the scale expected for waste vitrification (e.g., 3–15 MT/day), primarily because these glasses are relatively new. However, phosphate glasses have been successfully melted in commercial size furnaces in the US for several decades in the optical glass industry. Of more relevance to nuclear waste is that large quantities (2.2 million kg [10]) of a more chemically corrosive sodium–alumino phosphate glass has been successfully melted in Russia for up to six years in a JHM lined with commercial alumina–zirconia–silica (AZS) refractories as part of their waste vitrification effort.

The present work was motivated by the potentially significant savings in time and money that might be possible if the current JHM's, designed for melting borosilicate glass, could be used with minor modifications to vitrify the Hanford LAW in an iron phosphate glass. Consequently, the corrosion resistance of Inconel 690 and Inconel 693 in an iron phosphate melt containing 30 wt% of a simulated Hanford LAW has been studied to determine the suitability of these metals for electrodes in a JHM melting iron phosphate glass.

Inconel 690 was chosen since it is the current electrode material [11] being used in the JHM at DWPF to melt borosilicate glass. Inconel 693 was chosen since it is a modified version of Inconel 690, see Table 1, and might offer a higher corrosion resistance and longer service life.

Table 1
Composition and selected physical properties of Inconel 690 and 693 [12]

	Inconel 690[a]	Inconel 693[a]
Composition (wt%)		
Nickel	59.79	61.36
Chromium	30.06	28.87
Iron	9.14	5.83
Aluminum	0.34	3.27
Titanium	0.26	0.40
Carbon	0.033	0.019
Physical property		
Density (g/cm^3)	8.19	7.77
Melting range (°C)	1343–1377	1317–1367
Electrical resistivity (μΩm)	1.148	1.168

[a] Inconel 690 and 693 samples were supplied in the annealed condition by Special Metals Corporation [12].

2. Experiment

2.1. Preparation of glass

An iron phosphate glass was prepared which contained 30 wt% of the high sulfur Hanford LAW simulant and 70 wt% glass forming additives Fe_2O_3 and P_2O_5. The overall LAW simulant and batch compositions are given in Table 2. The appropriate amounts of the raw materials were mixed in a sealed plastic container for 30 min to produce a homogeneous mixture. This mixture was put in an alumina crucible and melted at 1050 °C for 2 h in an electric furnace in air. The melt was stirred 3–4 times with a fused silica rod over a period of 30 min to insure chemical homogeneity, and then poured onto the surface of a clean steel plate. The quenched glass was used for the corrosion tests.

2.2. Corrosion tests

Specimens (~14 mm × ~9 mm × ~7 mm) of Inconel 690 and 693 were cut from larger pieces of each metal using a diamond saw and then polished with 600 grit SiC paper by a polishing wheel. The dimensions and weight of each specimen were measured and recorded.

Fifty grams of the as-made iron phosphate glass was re-melted in an alumina crucible at 1050 °C for 30 min and then one Inconel specimen, which had been preheated to 1050 °C, was submerged in the melt. After a

Table 2
Nominal composition (wt%) of Hanford LAW simulant and batch containing 30 wt% LAW simulant

	LAW simulant	Batch
Al_2O_3	4.4	1.3
Cl	0.6	0.2
Cr_2O_3	0.4	0.1
F	1.6	0.5
Fe_2O_3	0.0	20.0
Na_2O	75.3	22.6
P_2O_5	7.7	52.2
SiO_2	0.5	0.2
SO_3	9.5	2.9
Total	100.0	100.0

prescribed time, the crucible was removed from the furnace and the Inconel sample was removed from the melt and immediately quenched in water. After cleaning and drying the Inconel sample, its weight was measured and the sample again submerged in the melt in the crucible and the corrosion test continued. The iron phosphate melt was replenished every 7 days with new as-made glass to minimize any compositional changes over the entire period of the test.

The weight of each specimen (initial weight 7.07 and 6.29 g for Inconel 690 and 693, respectively) was measured every 7 days, from which the weight loss of the sample was calculated as a function of time. The ratio of the weight difference (initial weight minus weight of specimen after a certain time interval) divided by the initial weight was defined as a percent weight loss at a given testing time. The corrosion tests were terminated after 155 days, whereupon, the final dimensions of each specimen were measured.

2.3. Analytical methods

A JEOL T330A scanning electron microscope (SEM) equipped with energy dispersive X-ray spectroscopy (EDS) operated at 15–20 kV was used to examine the external surface of the Inconel 690 and 693 specimens

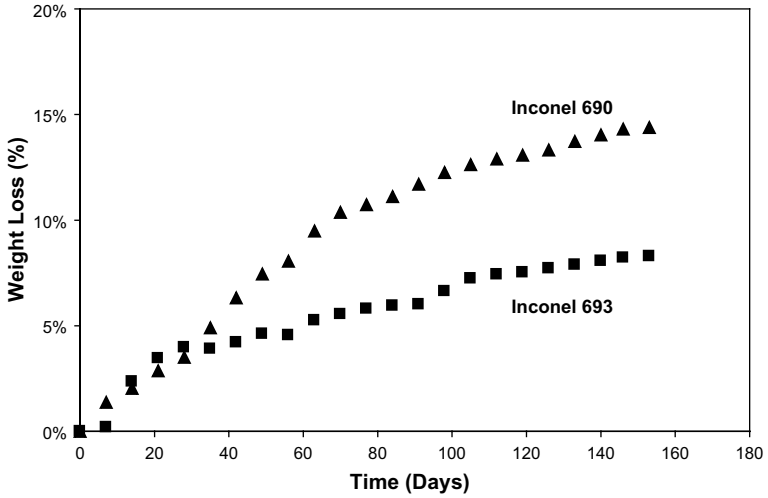

Fig. 1. Weight loss (%) of the submerged Inconel 690 and 693 samples as a function of time in an iron phosphate melt containing 30 wt% Hanford LAW at 1050 °C. Estimated error is represented by size of data points.

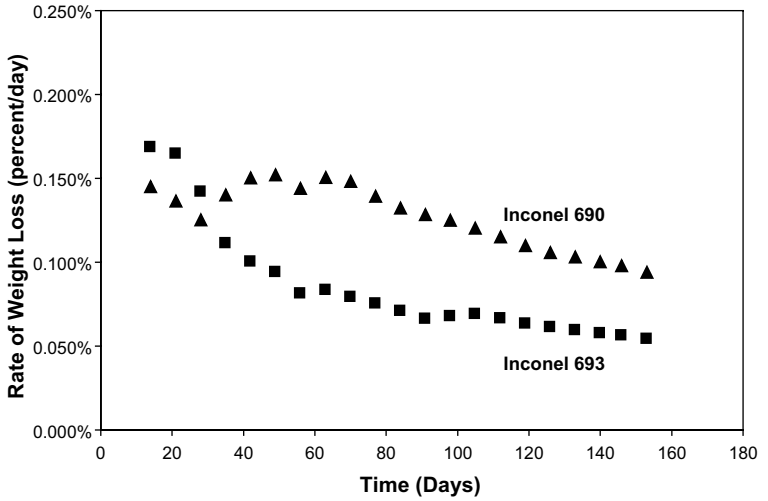

Fig. 2. Rate of weight loss (%/day) of the submerged Inconel 690 and 693 samples as a function of time in the iron phosphate melt containing 30 wt% Hanford LAW at 1050 °C. Estimated error is represented by size of data points.

after the 155 day corrosion test. A Scintag PADX X-ray diffractometer (XRD), Cu Kα radiation at a wavelength of 0.15418 nm, was used to identify any corrosion products (alteration phases) on the external surface of the metal samples after the corrosion test.

3. Results and discussion

3.1. Weight loss

The total weight loss after being submerged in the iron phosphate melt for 155 days was 14% and 8% for the Inconel 690 and 693 sample, respectively (Fig. 1). The calculated weight loss rate for the two samples as a function of time is shown in Fig. 2. The weight loss and its rate for Inconel 693 were about one half of that for Inconel 690, indicating that Inconel 693 was more chemically resistant to the melt.

The rate of weight loss for Inconel 690 and 693 was higher at the early stage of the corrosion test, and then gradually decreased with time. At the conclusion of the 155 day test, the weight loss rate was roughly two thirds and one third that of the initial rate for Inconel 690 and 693, respectively. This behavior is consistent with the formation of chemically protective layer which gradually formed on the external surface of the metal.

The corrosion rate of Inconel 690 and 693 was also determined by measuring the initial and final dimensions of the samples after the 155 day test. The overall corrosion rate (calculated by assuming a constant rate from time = 0) was 1.3 and 0.7 μm/day for the submerged Inconel 690 and 693 sample, respectively. These values are significantly smaller than the 6.5 μm/day rate reported [11] for the Inconel 690 electrodes in a JHM being used to melt borosilicate glass at 1150 °C in the DWPF at Savannah River. The typical appearance of the cross section of the submerged Inconel 693 sample after 155 days is shown in Fig. 3.

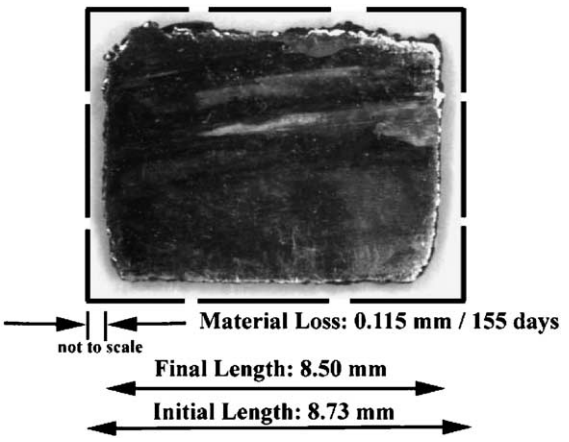

Fig. 3. Cross sectional view of the Inconel 693 sample after the corrosion test at 1050 °C for 155 days (0.115 mm/155 days = 0.7 μm/day). Note box around sample not to scale.

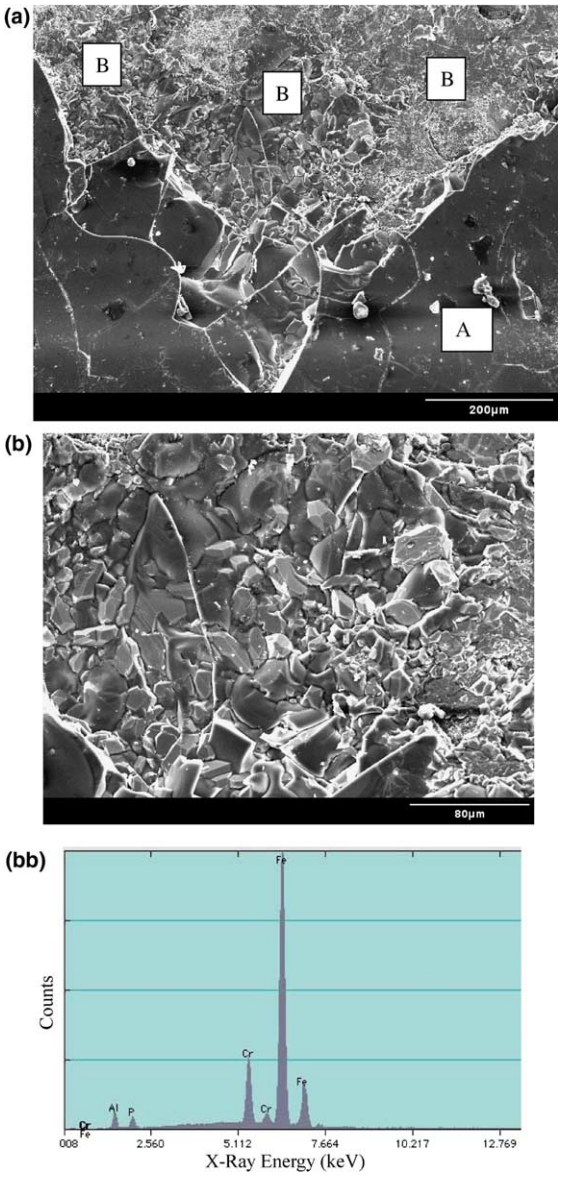

Fig. 4. (a) SEM micrograph of the external surface of the Inconel 690 sample after the 155 day corrosion test. A: residual glass attached to the surface; B: Fe-rich solid solution (Fe, Cr)$_2O_3$ alteration phase. (b) Close-up view of the Fe-rich (Fe, Cr)$_2O_3$ phase in area B. (bb) EDS spectra for the Fe-rich (Fe, Cr)$_2O_3$ phase.

3.2. Corrosion products

Only one alteration phase or corrosion product was found at the external surface of the Inconel 690 sample

submerged for 155 days in the iron phosphate melt containing 30 wt% Hanford LAW simulant. SEM micrographs and EDS spectra for this Fe-rich solid solution of (Fe, $Cr)_2O_3$ phase are shown in Fig. 4. Similarly, there was one main alteration phase at the surface of the Inconel 693 sample, but it was composed of crystals having two different morphologies (Fig. 5). There were smaller grain-like crystals such as those in Fig. 5(b) (Cr-rich solid solution of (Fe, $Cr)_2O_3$) and larger platy crystals, Fig. 5(c), (Fe-rich solid solution of (Fe, $Cr)_2O_3$). The presence of only the Fe-rich phase in the Inconel 690 sample may be due to its higher iron content

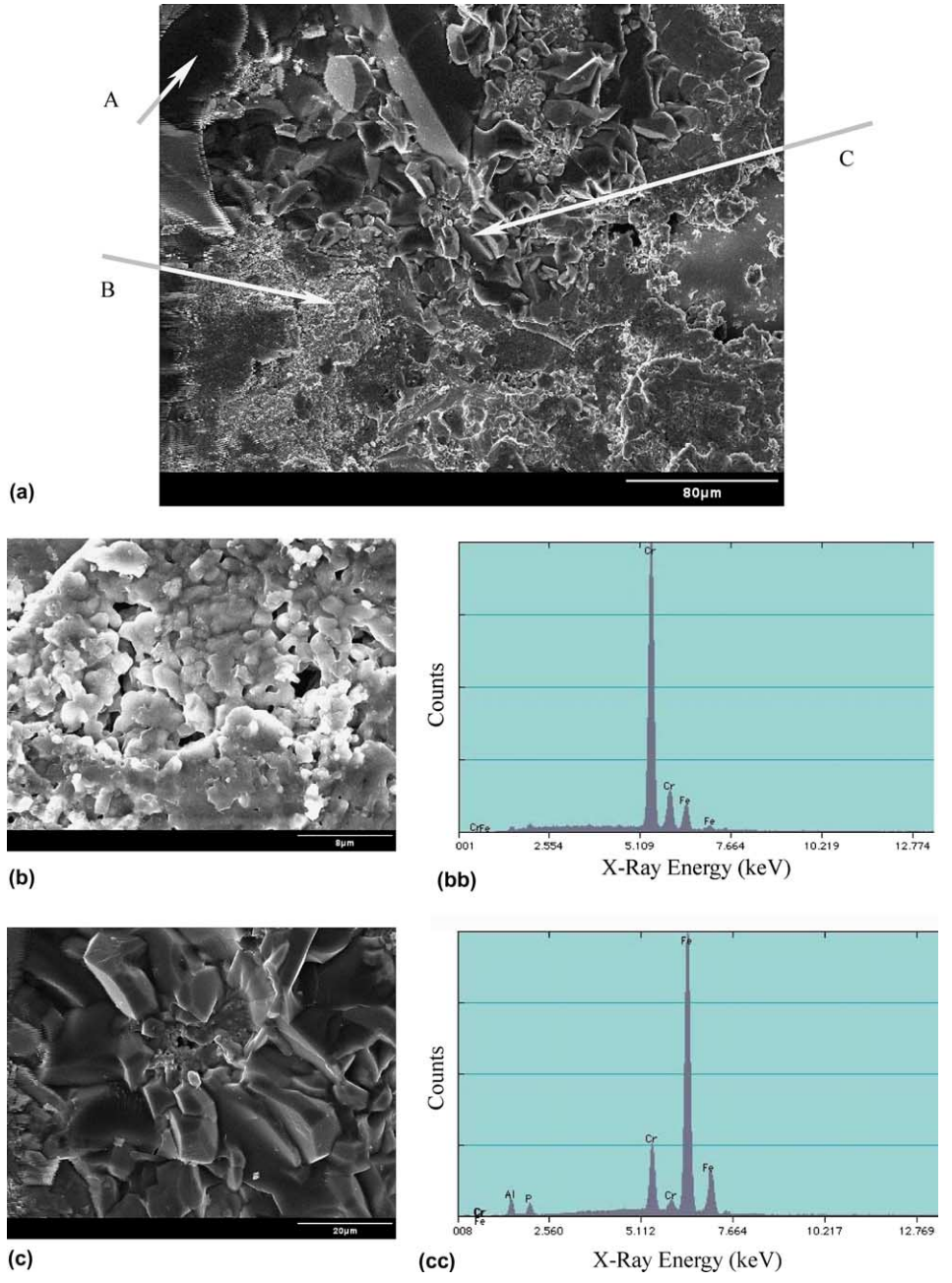

Fig. 5. (a) SEM micrograph of the external surface of the Inconel 693 sample after the corrosion test. A: residual glass attached to the surface; B: Cr-rich solid solution (Fe, $Cr)_2O_3$ alteration phase; C: Fe-rich solid solution (Fe, $Cr)_2O_3$ alteration phase. (b) Close-up view of the Cr-rich (Fe, $Cr)_2O_3$ phase in area B. (bb) EDS spectra for the Cr-rich (Fe, $Cr)_2O_3$ phase. (c) Close-up view of the Fe-rich (Fe, $Cr)_2O_3$ phase in area C. (cc) EDS spectra for the Fe-rich (Fe, $Cr)_2O_3$ phase.

(9.14 wt%) compared to the lower iron content (5.83 wt%) of Inconel 693, see Table 1. This suggests that iron corrodes more easily than chromium and that substituting other components such as Al and Ti for Fe in Inconel 693 (Table 1) enhances its corrosion resistance.

The XRD spectra of Inconel 690 and 693 before and after the corrosion test are shown in Fig. 6. The XRD Peaks for the Inconel 690 and 693 samples before corrosion were consistent with FCC alloys as expected. Diffraction peaks from the corroded samples of Inconel 690 and 693 corresponded to those for $(Fe, Cr)_2O_3$ (JCPDS-ICDD card # 02-1357). It should be noted that the diffraction peaks corresponding to the fresh Inconel alloys were also detected on the external surface of the corroded Inconel 693 sample (Fig. 6(b)-II), while these peaks were absent on the corroded Inconel 690 surface. The alteration layer (~20 μm) on the external surface of Inconel 693 was thinner and less extensive than that (~40 μm) formed on the Inconel 690 sample, see Fig. 7, implying that Inconel 693 was corroded less than 690.

No Ni-containing phase, such as $NiCr_2O_4$ (a Ni/Cr containing spinel) or $NiFe_2O_4$ (a Ni/Fe containing spinel), was detected on the surface of the corroded Inconel 690 and 693 samples, even though Ni was the main component (>53 wt%) in each metal. However, Ni was detected by X-ray fluorescence in the glasses after corrosion tests. These results suggest that all the Ni lost from the Inconel samples go into the glass melt rather than forming an alteration phase on the metals.

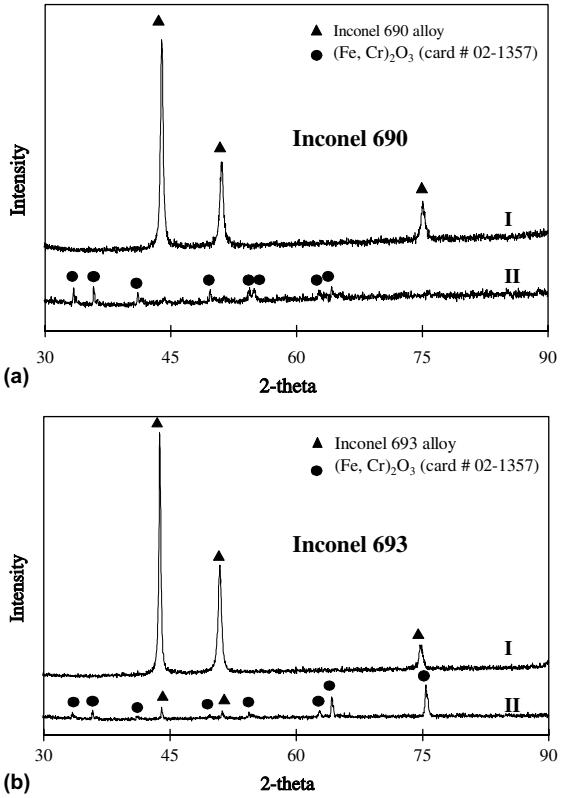

Fig. 6. (a) XRD spectra for the Inconel 690 sample before (I) and after (II) the corrosion test. (b) XRD spectra for the Inconel 693 sample before (I) and after (II) the corrosion test.

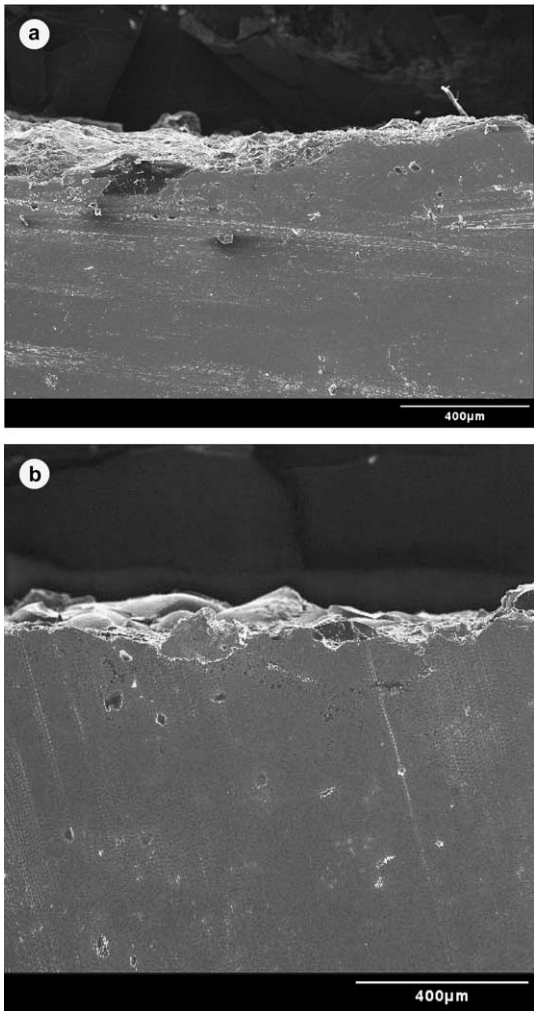

Fig. 7. SEM view of the cross section of the (a) Inconel 690 and (b) Inconel 693 sample after the corrosion test at 1050 °C for 155 days. Note that the alteration layer (~20 μm) of the Inconel 693 is thinner than that (~40 μm) of the Inconel 690.

4. Conclusions

The overall corrosion rate of Inconel 690 and 693 submerged for 155 days in an iron phosphate melt containing 30 wt% Hanford LAW stimulant at 1050 °C was small, 1.3 and 0.7 μm/day for Inconel 690 and 693, respectively. The corrosion resistance of Inconel 693

was about twice that of Inconel 690 in the iron phosphate melt as measured by the weight loss and dimensional changes.

The surface of both Inconels, at the completion of the corrosion test, was depleted in Ni and composed of a layer of $(Fe, Cr)_2O_3$. This layer appeared to act as a chemically protective layer on the metals.

These preliminary results are encouraging since the iron phosphate melt did not corrode the Inconel 690 to any greater extent than what has been reported for Inconel 690 electrodes in the borosilicate melt in the JHM at DWPF. Furthermore, Inconel 693 may be an even better candidate for use in iron phosphate melts since its corrosion rate was only about one half that of Inconel 690.

Acknowledgment

This work was supported by the Environmental Management Science Program of the US Department of Energy under contract FG07-96ER45618.

References

[1] US DOE, Summary Data on the Radioactive Waste, Spent Nuclear Fuel, and Contaminated Media Managed by the US Department of Energy, US Department of Energy, Washington DC (2001).
[2] J.D. Vienna, W.C. Buchmiller, J.V. Crum, D.D. Graham, D.-S. Kim, B.D. MacIsaac, M.J. Schweiger, D.K. Peeler, T.B. Edwards, I.A. Reamer, R.J. Workman, Pacific Northwest National Laboratory Report, PNNL-14050 (2002).
[3] D.S. Kim, W.C. Buchmiller, M.J. Schweiger, J.D. Vienna, D.E. Day, C.W. Kim, D. Zhu, T.E. Day, T. Neidt, D.K. Peeler, T.B. Edwards, I.A. Reamer, R.J. Workman, Pacific Northwest National Laboratory Report, PNNL-14251 (2003).
[4] C.W. Kim, D.E. Day, J. Non-Cryst. Solids 331 (2003) 20.
[5] Personal Communication, J.D. Vienna, Pacific Northwest National Laboratory (2004).
[6] H.D. Schreiber, C.W. Schreiber, E.D. Sisk, S.J. Kozak, Ceram. Trans. 45 (1994) 349.
[7] G.K. Sullivan, M.H. Langowski, P. Hrma, Ceram. Trans. 61 (1995) 187.
[8] H. Li, M.H. Langowski, P.R. Hrma, Ceram. Trans. 61 (1995) 195.
[9] C.W. Kim, D. Zhu, D.E. Day, D.S. Kim, J.D. Vienna, D.K. Peeler, T.E. Day, T. Neidt, Ceram. Trans. 155 (2004) 309.
[10] JCCEM Workshop, US/Russian Experiences on Solidification Technologies-Record of Meeting, Augusta, Georgia, September 4–5 (1997).
[11] Personal Communication, D.F. Bickford, Westinghouse Savannah River Company (2003).
[12] www.specialmetals.com.